

## Band Structure and Oscillatory Electron-Phonon Coupling of Pb Thin Films Determined by Atomic-Layer-Resolved Quantum-Well States

Yan-Feng Zhang,<sup>1</sup> Jin-Feng Jia,<sup>1</sup> Tie-Zhu Han,<sup>1</sup> Zhe Tang,<sup>1</sup> Quan-Tong Shen,<sup>1</sup> Yang Guo,<sup>1</sup> Z. Q. Qiu,<sup>2</sup> and Qi-Kun Xue<sup>1,\*</sup>

<sup>1</sup>Beijing National Laboratory for Condensed Matter Physics, Institute of Physics, The Chinese Academy of Sciences, Beijing 100080, China

<sup>2</sup>Departments of Physics, University of California at Berkeley, Berkeley, California 94720, USA

(Received 14 December 2004; published 26 August 2005)

Using a low temperature growth method, we have prepared atomically flat Pb thin films over a wide range of film thickness on a Si(111)- $7 \times 7$  surface. The Pb film morphology and electronic structure are investigated *in situ* by scanning tunneling microscopy and angle-resolved photoemission spectroscopy. Well-defined and atomic-layer-resolved quantum-well states of the Pb films are used to determine the band structure and the electron-phonon coupling constant ( $\lambda$ ) of the films. We found an oscillatory behavior of  $\lambda$  with an oscillation periodicity of two atomic layers. Almost all essential features in the Pb/Si(111) system, such as the growth mode, the oscillatory film stability, and the 9 monolayer envelope beating pattern, can be explained by our results in terms of the electron confinement in Pb films.

DOI: 10.1103/PhysRevLett.95.096802

PACS numbers: 73.21.Fg, 68.37.Ef, 79.60.Dp

As the film thickness is reduced to the range of electron Fermi wavelength ( $\lambda_F$ ), electrons moving in the normal direction of the film are quantized into the well-known quantum-well states (QWS) [1,2]. The discrete energy levels of the QWS greatly modulate the density of states of the electrons near the Fermi level ( $E_F$ ), and thus significantly affect the physical and chemical properties of a system. Because of the short  $\lambda_F$  in metals (for most metals,  $\lambda_F$  is  $\sim 1$  nm), a precise control of the film thickness is crucial to the formation of the well-defined QWS. In almost all previously studied metal-on-semiconductor or metal-on-insulator systems, it has been shown that it is extremely difficult to prepare atomically uniform ultrathin films over a macroscopic area due to crystal lattice mismatch and the different nature of atomic bonding [3,4].

Because the  $\lambda_F$  of Pb is about 4 times the lattice spacing ( $a_0$ ) along the (111) crystallographic direction, i.e.,  $\lambda_F \approx 4a_0$ , a thickness change of only one atomic layer is expected to produce a significant change in the electronic structure and other physical properties [5–8]. Angle-resolved photoemission spectroscopy (ARPES) plays a key role in characterizing and understanding the electronic structure and the quantum size effects (QSE) of Pb films [9,10]. However, most of the studies are either limited to the thinner thickness regime [ $< 10$  monolayers (ML)] or experiencing difficulty in controlling the film uniformity in the thicker regime as evidenced by the lack of a clear  $\sim 2$  ML oscillation in the density of states near the Fermi level. It is necessary to carry out photoemission experiments on atomically uniform Pb films over a wide thickness range.

Using a low temperature growth method, we prepared atomically flat Pb films on Si(111) over a wide thickness range (from 10 to 32 ML) and investigated the growth behavior and the electronic structure of the films by *in situ* scanning tunneling microscopy (STM) and ARPES. We

observed a fundamental 2 ML periodic film stability as well as an even-odd stability switching at every 9 ML increment. We demonstrate that this phenomenon is a direct consequence of the QSE. In addition, the well-defined and atomic-layer-resolved QWS energy spectra enable an accurate determination of the band dispersion near  $E_F$  and the electron-phonon coupling constant ( $\lambda$ ) of the films. We find that the  $\lambda$  also exhibits an oscillatory behavior due to the QSE.

A Si(111) substrate was prepared using the standard procedure in a molecular beam epitaxy system of a  $5 \times 10^{-11}$  Torr base pressure [11]. The growth chamber is connected to an analysis chamber where *in situ* STM (Omicron) and ARPES measurements can be performed for characterization of the film's surface morphology and electronic structure. The Pb film was grown on to the Si substrate at 145 K and the growth was monitored by reflection high-energy electron diffraction (RHEED). After the Pb deposition, the sample was warmed up gradually to room temperature and transferred to the analysis chamber. The photoemission spectra were collected by a SCIENTA SES-2002 Analyzer with a He I (21.2 eV) light source.

Real-time RHEED observation reveals that at 145 K uniform Pb films start to form at 6 ML, as evidenced by the long and sharp streaky RHEED pattern. After warming up the film to room temperature, for the films thinner than 10 ML the RHEED patterns become spotty, indicating that they are unstable, as further confirmed by room temperature STM observation. Above 10 ML, stable and atomically uniform Pb film is achieved at room temperature [Fig. 1(a)]. Although atomic steps exist on the surface, we find that the step density is the same as that on the Si(111) surface (we sampled more than 20 STM images from different regions on both the Pb and the Si surfaces), therefore the atomic steps on the Pb surface are due to the

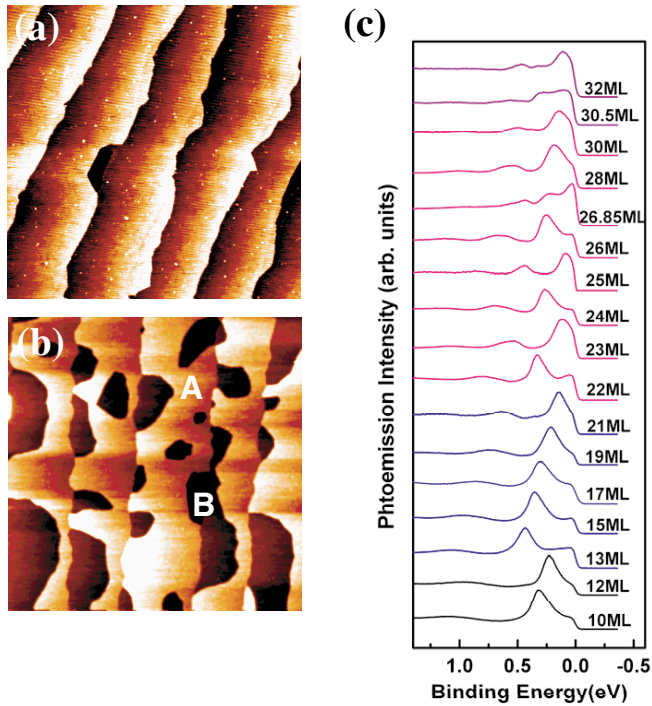


FIG. 1 (color). Room temperature STM images ( $2000 \text{ nm} \times 2000 \text{ nm}$ ) of the Pb films at the completion of 13 ML (a) and 14 ML (b). All stable films exhibit essentially the same morphology as that shown in (a), and are (111) oriented. In (b), the letter “A” indicates the 2 ML height islands on top of the 13 ML film labeled with the letter “B.” (c) Normal emission spectra measured at 110 K. The successive spectra have been graphically offset for clarity. Binding energy at 0.0 eV corresponds to the Fermi level.

atomic steps of the Si substrate. The uniformity of the Pb film is also evidenced by the photoemission data discussed below. From 10 to 21 ML, the growth proceeds via a novel double-layer mode; i.e., unstable films bifurcate into neighboring stable layers. This is clearly seen in Fig. 1(b) where a film with a nominal thickness of 14 ML is actually composed of a completely filled 13 ML film plus 2 ML height islands. A preferred thickness (a set point) appears at 13 ML where the stable thicknesses switch from even to odd layers. Such even-odd switching takes place at every 9 ML up to at least 32 ML. Above 21 ML, the preference for the even (odd) layer is no longer prominent and an essential layer-by-layer growth mode was observed.

To understand the above growth behavior, we performed an *in situ* photoemission experiment. Figure 1(c) displays the thickness-dependent photoemission spectra of the stable Pb films. Well-defined sharp QWS peaks within a 0.5 eV energy range below  $E_F$  are observed for all films studied, indicating again the high quality of the films [12]. A little nonuniformity of the Pb film will destroy the singularity of the QWS peaks, as shown in the spectra of 26.85 and 30.5 ML films in Fig. 1(c). For *s-p* metals the quantized energy levels are often described by the phase accumulation model [2],

$$2k(E)Nd + \phi_s(E) + \phi_i(E) = 2\pi n, \quad (1)$$

where  $k(E)$  is the electron wave vector along the  $\Gamma L$  (111) direction,  $\phi_s(E)$  and  $\phi_i(E)$  are the phase shifts of an electron upon reflection at the surface and the interface, respectively,  $n$  (an integer) is the QWS index,  $N$  is the number of atomic layers of the film, and  $d = 2.8435 \text{ \AA}$  is the lattice spacing along the  $\Gamma L$  direction [13].

Because the phase shift depends only on the electron energy, the wave vector  $k(E)$  at a given energy can be derived from the oscillation periodicity of the QWS at that energy without the need of the phase values. For example, if  $N_1$  and  $N_2$  correspond to the film thicknesses of two QWSs at the same energy ( $E$ ) with index  $n_1$  and  $n_2$ , it is easy to derive from Eq. (1) that

$$k(E) = \pi(n_2 - n_1)/[(N_2 - N_1)d]. \quad (2)$$

From the experimental data, we determined  $k(E)$ , the energy band of Pb, as shown in the insert of Fig. 2(a). The energy band near  $E_F$  exhibits an approximately linear relation between  $E$  and  $k$ . Since this energy band comes from band folding from the second Brillouin zone (BZ), we fit the band using  $E = -\frac{\hbar^2(2k_{BZ} - k_F)}{2m_e}(k - k_F)$ . The fitting

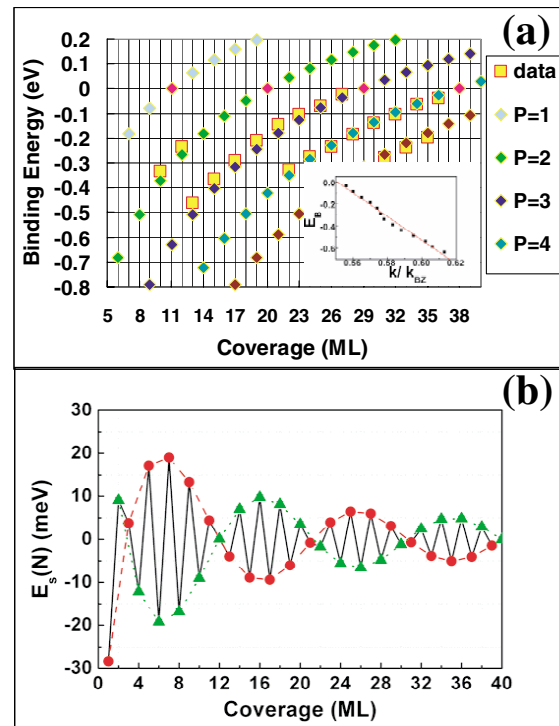


FIG. 2 (color). (a) Binding energy of the QWS as a function of Pb film thickness (the shadowed squares and diamonds correspond to the experimental and the fitting results, respectively). For each measured “branch” of QWS in the photoemission data, the reduced quantum member  $P$  is indicated at the right panel of the figure. The inserted panel shows the experimentally determined energy band  $E(k)$  along the  $\Gamma L$  direction in the first Brillouin zone. (b) Calculated relative surface energy as a function of the film thickness.

yields an effective electron mass of  $m_e^* = 1.2m_e$  ( $m_e$  is the free electron mass) and a Fermi wave vector of  $k_F = 0.611 \text{ \AA}^{-1}$ , or  $k_F' = 2k_{BZ} - k_F = 1.598 \text{ \AA}^{-1}$  before the band folding, which is very close to the value of  $1.596 \text{ \AA}^{-1}$  obtained from the de Haas–van Alphen measurement in the extended Brillouin zone scheme [13,14].

We fit the QWS in the  $E$ - $d$  plane [Fig. 2(a)] by assuming a linear dependence of the total phase shift on the energy; i.e.,  $\phi_s + \phi_i = \pi(a^*E + b)$ . The fitting result (diamonds) is in excellent agreement with the experimental results (shadowed squares).

The value of  $k_F = 0.611 \text{ \AA}^{-1}$  leads to a Fermi level crossing of the QWS at every  $\Delta N = \pi/k_F d$  (ML) = 1.8 ML, in agreement with a previous theoretical calculation [15]. This result is also consistent with the photoemission data in Fig. 1(c) that the highest occupied QWS above 21 ML oscillates (with respect to  $E_F$ ) with a nearly 2 ML periodicity. The 2 ML oscillation was recently shown to result in a spectacular oscillatory superconductivity transition temperature [16].

The small difference between  $2k_F$  and  $k_{BZ}$  generates a “beating effect” with an oscillation periodicity of  $\pi/(2k_F - k_{BZ}) = 9$  ML [15]. Indeed, it can be observed in Fig. 2(a) that the QWS labeled with index  $P$  (defined as  $P \equiv 3N - 2n$ ) crosses  $E_F$  with an exact 9 ML periodicity. We also observe that as the QWS of an odd (even) branch  $P$  crosses  $E_F$ , there is a switching of the film stability from odd (even) to even (odd) layers. This even-odd switching occurs at 13, 22, and 31 ML, respectively, with an interval of 9 ML. In particular, the film becomes most unstable if a QWS is right at  $E_F$ . This situation appears at 11, 20, 29, and 38 ML [see Fig. 1(c)], again with an interval of 9 ML.

From our experiment, we see that for  $P = 2$  (10 ML, 12 ML) and  $P = 3$  (13 ML, 15 ML, 17 ML, 19 ML, 21 ML), the occupied QWS of the stable films have a lower energy than their adjacent unstable layers. This observation explains the preference of the even (odd) layers of the stable films. The energy difference between the odd and even layers decreases with increasing film thickness, and eventually leads to a quasi-layer-by-layer growth above 21 ML.

Relative surface energy calculation [17] provides a good understanding of the relative film stability at different thicknesses. Using the experimental results, we calculated the surface energy of the Pb films in a Friedel form [18]

$$E_s(N) = A \frac{\cos[2k_F(N + \Delta N)d]}{(N + \Delta N)^\alpha} + B, \quad (3)$$

where  $k_F = 1.598 \text{ \AA}^{-1}$  is deduced from our experiment,  $d = 2.8435 \text{ \AA}$  is the atomic-layer spacing,  $\alpha = 0.938$ , and  $A$  and  $B$  are constants.  $\Delta N$  is the additional nominal thickness caused by the quantum well change associated with the charge transfer between the Pb overlayer and the substrate [7]. As shown in Fig. 2(b), Eq. (3) represents a damped sinusoidal function with a Friedel oscillation wavelength that is half of the Fermi wavelength (1.8 ML

in the present case) [19], riding on an envelope beating function with a 9 ML internode distance. The film stability and the growth behavior observed in our experiments are consistent with this calculation.

Formation of QWSs not only modulates the density of states near  $E_F$ , but also causes mechanical expansion/shrinkage of the film lattice in the growth direction [7] which could modulate the  $\lambda$ . We performed a temperature-dependent photoemission experiment to deduce the  $\lambda$  using the method reported in previous studies [20–22]. Normal emission spectra of even (22 ML) and odd (23 ML) layers at different temperatures are shown in Figs. 3(a) and 3(b) respectively. The linewidths ( $\Delta E$ ), deduced from curve fitting as Voigt profile with Lorentzian line shape of the two typical films, are plotted in Fig. 4(a). We see that the  $\Delta E$  of both films increases linearly with increasing temperature but with prominent different slopes. The slope is related to  $\lambda$  via

$$\lambda = \frac{1}{2\pi k_B} \frac{d\Delta E}{dT}. \quad (4)$$

Figure 4(b) (triangles) shows the  $\lambda$  values derived from the QWS peaks at different film thicknesses. Besides an overall gradual increase of the  $\lambda$  value toward its bulk value (1.55) [23], an oscillation of  $\lambda$  is clearly seen. The oscillatory  $\lambda$  was previously reported in a Ag/Fe(100) system. This phenomenon was attributed to the QWS phase variation at the interface [22]: those states with an antinode at the interface should have a greater overlap of the QWS wave function with the interfacial potential thus to induce a greater electron-phonon coupling. We believe that the oscillation of  $\lambda$  in our study originates from the same mechanism. The superconducting transition temperature ( $T_c$ ) of the Pb film was also calculated with the measured  $\lambda$  value using the Eliashberg-McMillan formula [diamonds in Fig. 4(b)] and compared with our previous experimental result (balls) [16]. Although a direct relationship between  $\lambda$  and  $T_c$  is unknown, the same oscillatory behavior of  $\lambda$  and  $T_c$  indicates that they are both induced by the QSE.

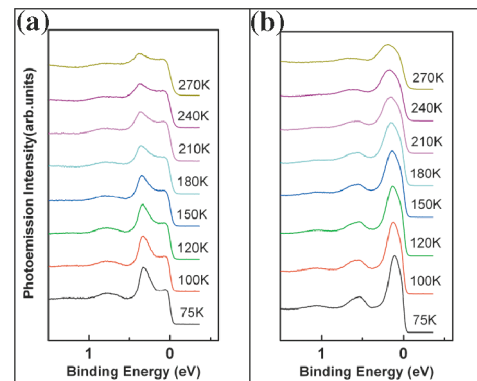


FIG. 3 (color). Temperature-dependent photoemission spectra (75–300 K) obtained from both even (22 ML) (a) and odd (23 ML) (b) layered films.

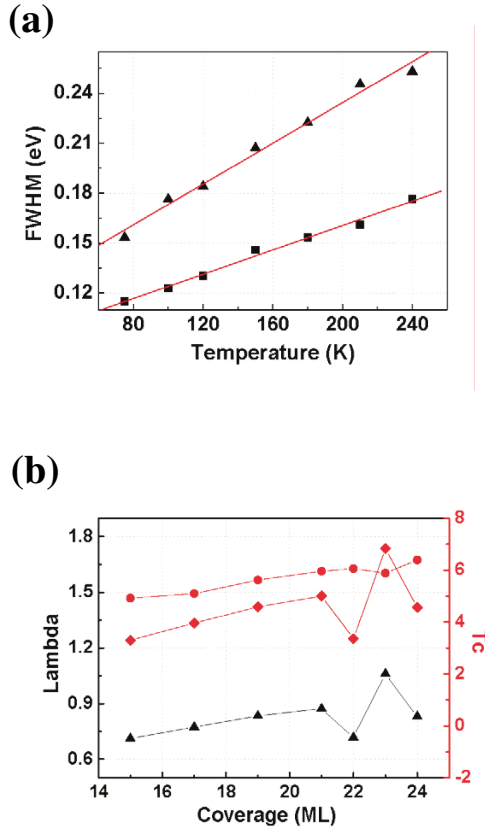


FIG. 4 (color). (a) Lorentzian peak widths of the QWS of the 22 (square) and 23 ML (triangle) films as a function of the sample temperature. (b) Measured  $\lambda$  (triangles) as a function of the film thickness, and the calculated superconductivity transition temperature (diamonds) by the formula  $T_c = \frac{\Theta_D}{1.45} \times \exp\left[-\frac{1.04(1+\lambda)}{\lambda - \mu^* - 0.62\lambda\mu^*}\right]$  [24]. In the calculation, typical values of 0.1 for  $\mu^*$  (the effective Coulomb interaction) and 105 K for  $\Theta_D$  (the Debye temperature) were used. As a comparison, the experimental transition temperature of the Pb films covered with 4 ML Au is also displayed (balls).

Since many properties, such as resistivity, structure, and specific heat, depend strongly on  $\lambda$  [24], the present measurement provides useful information for understanding how QSE affects the physical properties of the Pb films.

In summary, atomically uniform Pb thin films are achieved in a wide thickness range (from 10 to 32 ML) on Si(111) surface. The energy dispersion near  $E_F$ , the effective electron mass, the Fermi wave vector, and the electron-phonon coupling constant are determined. We show that the electron confinement plays a dominant role in the observed novel growth mode, oscillating film stability, and the electron-phonon coupling strength. Such uniform films form an ideal 1D finite potential well prototype

for exploring novel physical phenomena associated with QSE.

Work in Beijing was financially supported by NSF and MOST of China. Z. Q. Qiu is grateful for the support of NSF DMR-0405259.

\*Electronic address: qkxue@aphy.iphy.ac.cn

- [1] J.J. Paggel, T. Miller, and T.-C. Chiang, *Science* **283**, 1709 (1999).
- [2] T.-C. Chiang, *Surf. Sci. Rep.* **39**, 181 (2000); M. Milum, P. Pervan, and D.P. Woodruff, *Rep. Prog. Phys.* **65**, 99 (2002).
- [3] J. Walz *et al.*, *Appl. Phys. Lett.* **73**, 2579 (1998).
- [4] A. Grossmann, W. Erley, J.B. Hannon, and H. Ibach, *Phys. Rev. Lett.* **77**, 127 (1996).
- [5] I. B. Altfeder, K. A. Matveev, and D. M. Chen, *Phys. Rev. Lett.* **78**, 2815 (1997).
- [6] W.B. Su *et al.*, *Phys. Rev. Lett.* **86**, 5116 (2001); V. Yeh *et al.*, *Phys. Rev. Lett.* **85**, 5158 (2000); M. Hupalo and M.C. Tringides, *Phys. Rev. B* **65**, 115406 (2002); K. Budde, E. Abram, V. Yeh, and M.C. Tringides, *Phys. Rev. B* **61**, R10602 (2000).
- [7] P. Czoschke, Hawoong Hong, L. Basile, and T.-C. Chiang, *Phys. Rev. Lett.* **91**, 226801 (2003).
- [8] I. Vilfan, M. Henzler, O. Pfennigstorf, and H. Pfnür, *Phys. Rev. B* **66**, 241306 (2002).
- [9] A. Mans, J.H. Dil, A.R.H.F. Ettema, H.H. Weitering, *Phys. Rev. B* **66**, 195410 (2002).
- [10] M.H. Upton *et al.*, *Phys. Rev. Lett.* **93**, 026802 (2004).
- [11] Jian-Long Li *et al.*, *Phys. Rev. Lett.* **88**, 066101 (2002).
- [12] D.R. Heslinga *et al.*, *Phys. Rev. Lett.* **64**, 1589 (1990).
- [13] J.R. Anderson and A.V. Gould, *Phys. Rev.* **139**, A1459 (1965).
- [14] M. Jalochowski, H. Knoppe, G. Lilienkamp, and E. Bauer, *Phys. Rev. B* **46**, 4693 (1992).
- [15] C.-M. Wei and M.Y. Chou, *Phys. Rev. B* **66**, 233408 (2002).
- [16] Y. Guo, Y.F. Zhang, X.Y. Bao *et al.*, *Science* **306**, 1915 (2004).
- [17] J.C. Boettger *et al.*, *J. Phys. Condens. Matter* **10**, 893 (1998).
- [18] P. Czoschke, Hawoong Hong, L. Basile, and T.-C. Chiang, *Phys. Rev. Lett.* **93**, 036103 (2004).
- [19] Z. Zhang, Q. Niu, and C.-K. Shih, *Phys. Rev. Lett.* **80**, 5381 (1998).
- [20] B.A. McDougall, T. Balasubramanian, and E. Jensen, *Phys. Rev. B* **51**, 13 891 (1995).
- [21] M. Kralj *et al.*, *Phys. Rev. B* **64**, 085411 (2001).
- [22] D.-A. Luh, T. Miller, J.J. Paggel, and T.-C. Chiang, *Phys. Rev. Lett.* **88**, 256802 (2002).
- [23] J.P. Carbotte, *Rev. Mod. Phys.* **62**, 1027 (1990).
- [24] G. Grimvall, *The Electron-Phonon Interaction in Metals* (North-Holland, New York, 1981).